Accurate Measurements of the Nuclear Processes $T(p,p)T$, $T(p,^3He)n$, $T(p,d)D$, and $T(\vec{p},\hat{p})T$ from 13 to 20 MeV*

J. L. Detch, Jr.,† R. L. Hutson, Nelson Jarmie, and J. H. Jett

Los Alamos Scientific Laboratory, University of California, Los Alamos, New Mexico 87544

(Received 1 April 1971)

Differential cross sections have been measured with absolute accuracies of about 1.0% and relative accuracies of about 0.7% using a tritium gas target with thin foil windows and a silicon surface-barrier detector telescope in conjunction with an on-line computer for mass identification and data handling. The angular scattering distributions for $T(p,p)T$, $T(p,d)D$, and $T(p,^3He)n$, and the proton asymmetries of $T(\vec{p},\hat{p})T$ were measured at a proton laboratory energy of 13.600 MeV. In addition, differential cross sections for $T(p,p)T$ were measured at energies of 16.230 and 19.480 MeV to provide supporting data for existing mass-4 studies at these energies.

Related data are compared and preliminary attempts to analyze the data with an energy-independent phase-shift-analysis program are discussed. Several sets of single-channel phase-shift solutions are given for maximum angular momentum L values of 3. These solutions are not unique. Simultaneous two- and three-channel analyses have been inconclusive.

Polarization asymmetry measurements using the Los Alamos Scientific Laboratory Lamb-shift polarized ion source show a maximum analyzing power of about +0.70 at 13.600 MeV for $T(\vec{p},\hat{p})T$. These values are related to existing analyzing power measurements of $^3He(\vec{p},\hat{p})^3He$ and $T(\vec{p},\hat{p})T$ near this energy.

I. INTRODUCTION

The region of very light nuclei remains one of the least understood regions of the table of nuclides. The application of simple nuclear models, the use of the two-nucleon force directly, or even phase-shift analyses has had limited success.

In recent years a sizable theoretical effort has been made toward understanding the mass-4 system by Meyerhof and McElearney,[1] Werntz,[2] Tombrello,[3] Dodder,[4] and others, but has been hampered by the lack of accurate experimental data over suitable energy ranges to provide good experimental comparison. Experiments using tritium as the target material are particularly limited, primarily due to the problems inherent with the handling of a radioactive gas. In the energy range of 10 to 20 MeV there exist few data obtained using tritium as the target medium and protons for the bombarding particle. The cross-section data which exist are inadequate to obtain unique phase-shift solutions.

We bombarded tritium with energetic protons and measured accurate (~0.8% scale errors, ~0.7% relative errors) differential cross sections for $T(p,p)T$, $T(p,d)D$, $T(p,^3He)n$, and the analyzing power of $T(\vec{p},\hat{p})T$ at 13.600 MeV. In addition, we measured the elastic scattering angular distributions of $T(p,p)T$ at 16.230 and 19.480 MeV. These data should prove to be beneficial to the phase-shift analysis of proton-triton scattering and reactions in a twofold manner. First, they provide a consistent set of accurate data for the elastic and reaction channels which are necessary to help eliminate spurious phase-shift solutions of the elastic scattering data. Second, our data provide a consistent set of accurate cross sections over a moderate energy range. The reasonable behavior of a set of phase shifts as a function of energy may allow one to eliminate additional spurious phase-shift solutions.

Vanetsian and Fedchenko[5] reported differential cross sections for $T(p,p)T$ at a proton energy of 19.48 MeV, though the values which they reported (only available from a small graph) are generally regarded with skepticism and their numerical values are unavailable. We repeated this experiment at 19.480 MeV, and indeed found large discrepancies (~50%) with some of their values. Rosen and Leland measured cross sections[6] for $T(p,p)T$ at 14.6 MeV and measured the analyzing power[7] of $T(\vec{p},\hat{p})T$ at 14.5 MeV. Our data are in general agreement with that of Rosen and Leland and provide improved accuracy necessary for obtaining smaller uncertainties in the phase-shift parameters. In addition, our energies were chosen so that our data would supplement existing $^3He(p,p)^3He$ data and phase-shift analyses by Tivol[8] and Hutson *et al.*[9,10] This is the extent of the $T(p,p)T$ elastic scattering and proton analyzing power known at the present time in the energy range of 10 to 20 MeV.

At 13.600 MeV we measured the differential scattering cross sections for the reaction $T(p,d)D$.

Rosen and Leland[6] measured the $T(p,d)D$ reaction near 14.5 MeV; their data are unpublished. We are unaware of any other measurements of this reaction in the energy range of 10 to 20 MeV. However, there exist data on the inverse reaction of $D(d,p)T$ at 12.15 and 13.8 MeV by Brolley, Putnam, and Rosen.[11] The principle of detailed balance[12] may be applied to these data to obtain indirectly cross-section data for the reaction $T(p,d)D$. Though the standard errors of the Brolley, Putnam, and Rosen[11] data are 3 to 4%, these data compare favorably with our own.

By detecting the recoiling helium-3 particle we were able to obtain a partial angular scattering distribution for the reaction $T(p,{}^3He)n$ at 13.600 MeV. The equivalent reaction of $T(p,n)^3He$ has been more extensively investigated by others as a source of neutrons. Neutron production total and relative differential cross sections above 10 MeV have been reported by Bogdanov *et al.*,[13,14] Goldberg *et al.*,[15,16] Wilson, Walter, and Fossan,[17] and Dietrich and Meyerhof[18] with varying degrees of success in their absolute normalizations. By detecting the charged helium-3 particle in the $T(p,{}^3He)n$ reaction, we provide a more reliable absolute normalization for this reaction cross section at 13.600 MeV. Partial angular distributions for the neutron polarization resulting from the bombardment of tritium with polarized protons are given by Seagrave,[19] Barschall,[20] Walter *et al.*,[21,22] and Alekseev *et al.*,[23] though there appears to be some degree of inconsistency between several pieces of these data.

Additional references to existing data outside the range of 10 to 20 MeV and to other related reactions are given by Meyerhof and Tombrello.[24] An early report of our work is given in Ref. 25 for the $T(\vec{p},\hat{p})T$, and Ref. 26 for the cross sections. The entire work is expanded in detail in a thesis.[27]

II. EXPERIMENTAL EQUIPMENT AND PROCEDURE

Experimental equipment and running procedure are discussed in great detail by Detch[27] and Jarmie *et al.*[28] Only items special to this experiment will be discussed at length. Protons from the Los Alamos Scientific Laboratory (LASL) electrostatic accelerator system entered a precision scattering chamber and were used to bombard a tritium gas target with thin foil windows. The recoil fragments were detected by a solid-state detector telescope; the resulting signals were refined by a simple electronic system and passed into an on-line computer for mass analysis and data handling.

The tritium used was stored as uranium tritide and was liberated by heating when needed. The target gas was purified with the use of an activated charcoal trap just before filling the target. The result was a target gas with contaminants other than hydrogen of less than 1%. Target purity decreased roughly 1% per 24 h that the target was filled, an effect due largely to exchange of the tritium with hydrogen contained in organic contaminants in the target system. The purity was determined by measurement of the contaminant scattered protons along with information from mass-spectrographic analysis of the target gas. The purity of the target gas was obtained by combining the fractional contaminations of hydrogen, deuterium, and other gases such as carbon, oxygen, and nitrogen. The target was typically operated at 175 Torr with 90 to 95% pure tritium.

In obtaining the data on the proton polarization asymmetries, the Los Alamos Lamb-shift polarized ion source[29] was utilized as an injector into the tandem Van de Graaff accelerator. This ion source provided spin-polarized protons of approximately 90% polarization in the form of negative hydrogen ions.

At the time our polarization data were taken, the polarized ion source was producing 180 nA of 90% polarized protons, with approximately 20 nA of beam current arriving on target. Subsequent modification to the ion source has greatly increased the output, and other experimenters have reported beam currents in excess of 100 nA of 90% polarized protons *on target*. This high beam current of polarized protons makes feasible various experiments which would have been previously extremely difficult.

The polarized ion source employed an "rf quench"[29] method of measuring the beam polarization. The beam polarization supplied by this method was calibrated against the known[30] analyzing power of helium-4 by running with the target filled with helium at the backward-angle maximum of the p-^4He analyzing power at 13.6 MeV. The calibrated value was higher than the measured value by $1.0\% \pm 1.0\%$ (see Sec. III), limited primarily by statistical uncertainties. The comparison of these two methods provided a check on the measure of the beam polarization and should have revealed any gross geometrical asymmetries in the detector equipment.

At each polar angle, four cross-section measurements were made. With the spin oriented in the "up" direction, the cross sections were measured in the left and right scattering directions. The spin was then flipped with a spin precessor to provide a "spin-down" beam, and the measurements were repeated in the right and left scatter-

ing directions. The Basel convention for algebraic sign of the scattering asymmetry uses a "spin-up" beam direction and defines the asymmetry quantity, $(\sigma_L - \sigma_R)/(\sigma_L + \sigma_R)$, where σ_L is the observed cross section for scattering to the left, and σ_R is the observed cross section for scattering to the right. The first two of our four measurements determine this quantity for the asymmetry. By inverting the polarization direction to provide "spin down," and measuring the equivalent quantity $(\sigma_R - \sigma_L)/(\sigma_R + \sigma_L)$, it is possible to combine these two asymmetries and eliminate false geometric asymmetries in the detector apparatus (see Ref. 27). The combined "up-vs-down" measurements were used to obtain the $T(\vec{p}, \hat{p})T$ proton analyzing power, by dividing the measured asymmetry by the beam polarization. Measurements of the beam polarization were made[29] before and after each cross-section measurement.

This type of experiment is usually done with two detectors, one on the left and one on the right of the beam direction. However, analysis of the errors[31] involved showed that in view of the high mechanical accuracy of our scattering apparatus, double detectors would double the counting rate, but would not significantly decrease the errors caused by false-geometry asymmetries or other systematic effects. The significant errors in our proton analyzing-power measurements are due to uncertainties in the beam polarization and due to statistical uncertainties.

III. ERRORS

Sources of error are discussed in detail in Refs. 27 and 28. Only contributions to error that are peculiar to this experiment will be reviewed. The major difference is in the use of tritium as a target gas, and the difficulty in determining the purity of this gas as previously discussed. The error in the knowledge of the purity of the tritium (90–95%) varied from 0.6% to 2.0%. This error dominated the uncertainty in the number of scattering centers and in the scale (over-all normalization) error. The problem of determining the purity is the cause for the data being grouped in sets each with its own scale error, this being the result of running the experiment with several fillings of target gas. The contributions to the scale error, i.e., the absolute normalization error, include errors in N_T (due to pressure, temperature, and purity uncertainties), N_b, and G. Contributions to the relative and scale errors are combined in quadrature to give the absolute error according to

$$(\text{Abs. error})^2 = (\text{Scale error})^2 + (\text{Rel. error})^2 .$$

Table I contains a summary of the various sources of error which are not negligible in the cross sections.

The central energy of the proton beam used was known to ±15 keV and had an energy spread of 20 keV full width at half maximum (FWHM), including the effects of foil and target gas straggling and machine energy resolution. The error in the analyzing power is discussed in detail in Sec. 5.2 of Ref. 27. The relative error is dominated by the statistical error.

There is also a fractional scale error in the beam polarization of 1.0% coming from the p-α calibration (see Sec. II). The calibration assumes a maximum p-α analyzing power of 1.0. This assumption appears as if it will be very good. We have taken p-α phase shifts from the work of Satchler *et al.*[30] and also from the recent energy-dependent analysis of Arndt, Roper, and Shotwell.[32] These phases predict maximum p-α polarization at or near 13.6 MeV of 0.999 or greater. This error contributes a corresponding fractional scale error in the analyzing power. Since in much of the data the analyzing power is small, the absolute contribution of this scale error is small.

IV. DATA

A. T(p, p)T Differential Cross Sections at 13.600, 16.230, and 19.480 MeV

Laboratory and center-of-mass differential cross sections for the elastic scattering of $T(p, p)T$ at 13.600, 16.230, and 19.480 MeV are listed in Tables II–IV, respectively. Relative and scale errors are presented as standard deviations. The relative errors relate the relative values of the data within a given group. The relationship of data in different groups must take into account the scale errors of the groups. The beam energy is known to ±15 keV with a spread of 20 keV FWHM.

$T(p, p)T$ center-of-mass differential cross sections are presented graphically in Figs. 1–3 for the energies of 13.600, 16.230, and 19.480 MeV, respectively. Error bars are not shown on these graphs as the errors are approximately $\frac{1}{4}$ the size of the plotting dots used on the graphs.

TABLE I. Error summary.

Scale		Relative	
Source	% Error	Source	% Error
Pressure	0.1	Yield	$100/\sqrt{Y}$
Temperature	0.07	Background	~0.1
Purity	0.6–2.0	Dead time	0.0–0.6
G	0.2		
N_b	0.2		

B. $T(\vec{p}, \hat{p})T$ Proton Analyzing Power at 13.600 MeV

The proton analyzing power of $T(\vec{p}, \hat{p})T$ at 13.600 MeV is presented with error evaluations in Table V. The errors given are relative errors; the scale error is discussed in Sec. III. Our $T(\vec{p}, \hat{p})T$ analyzing power at 13.600 MeV is presented graphically in Fig. 4, along with similar data by Leland and Rosen[7] at 14.5 MeV for comparison. Error bars are deleted when errors are exceeded by the size of the plotting dots.

C. $T(p, d)D$ Differential Cross Sections at 13.600 MeV

Laboratory and center-of-mass differential cross sections for the reaction $T(p, d)D$ at 13.600 MeV are listed in Table VI with relative and scale errors (standard deviations). The relative error relates the data within a given group. The relative error relating data in *different* groups is the absolute error. The beam energy is known to ±15 keV with a spread of 20 keV FWHM. This listing represents the cross section for observing a (either) deuteron, and is a factor of 2 larger than the cross section quoted by some authors.

TABLE II. $T(p, p)T$ differential cross sections at 13.600 MeV.

θ_{lab} (deg)	σ_{lab} (mb/sr)	$\theta_{c.m.}$ (deg)	$\sigma_{c.m.}$ (mb/sr)	Relative error (%)	Scale error (%)
10.00	509.5	13.36	287.3	1.71	0.77
12.00	519.3	16.03	293.9	1.00	for
15.00	499.5	20.01	284.6	0.60	entire
20.00	450.7	26.63	260.7	0.55	group
25.00	394.8	33.20	232.8	0.52	
30.00	336.7	39.71	203.3	0.52	
35.00	274.0	46.16	170.0	0.50	
40.00	215.6	52.52	138.1	0.50	
45.00	166.4	58.79	110.5	0.52	
50.00	128.6	64.97	88.90	0.55	
55.00	95.57	71.03	68.97	0.54	
60.00	67.67	76.97	51.18	0.55	
65.00	46.36	82.78	36.88	0.78	
70.00	31.02	88.45	26.03	0.60	
75.00	20.50	93.98	18.19	0.82	
80.00	12.87	99.36	12.11	0.66	
90.00	5.545	109.66	5.893	1.09	
100.00	5.231	119.34	6.305	1.17	
110.00	8.424	128.42	11.50	0.84	
120.00	13.48	136.92	20.75	0.65	
130.00	19.26	144.92	33.06	0.53	
140.00	24.26	152.47	45.82	0.53	
150.00	28.01	159.67	57.19	0.50	
160.00	30.83	166.60	66.68	0.48	
165.00	32.14	169.99	70.95	0.50	
168.00	32.08	172.00	71.51	1.00	

$T(p, d)D$ center-of-mass differential cross sections at 13.600 MeV are presented graphically in Fig. 5. Errors are exceeded by the size of the plotting dots and error bars are deleted. As identical particles comprise the outgoing channel, the data should be symmetric about 90° in the center-of-mass system. The solid circles represent the data. The open squares represent the data points reflected about 90° in the center-of-mass system and are plotted for comparison.

D. $T(p, {}^3He)n$ Differential Cross Sections at 13.600 MeV

Laboratory and center-of-mass differential cross sections for the reaction $T(p, {}^3He)n$ at 13.600 MeV are listed in Table VII with relative and scale errors (standard deviations). The scale normalization error is combined in quadrature with the relative error to yield the absolute error. The beam energy is known to ±15 keV with a spread of 20 keV FWHM.

Major contributions to the errors for data at angles greater than 80° in the center-of-mass system were due to uncertainties in the background subtraction. Due to the low energy of the

TABLE III. $T(p, p)T$ differential cross sections at 16.230 MeV.

θ_{lab} (deg)	σ_{lab} (mb/sr)	$\theta_{c.m.}$ (deg)	$\sigma_{c.m.}$ (mb/sr)	Relative error (%)	Scale error (%)
12.00	450.5	16.03	254.6	0.70	0.77
15.00	438.6	20.02	249.7	0.60	for
20.00	397.5	26.64	229.7	0.54	this
25.00	345.5	33.22	203.6	0.53	group
30.00	286.4	39.73	172.8	0.52	
35.00	230.3	46.18	142.8	0.53	
40.00	179.0	52.55	114.6	0.52	
40.00	179.2	52.55	114.7	0.71	0.77
45.00	138.4	58.82	91.86	0.80	for
50.00	102.1	64.99	70.54	0.75	this
55.00	73.76	71.06	53.21	1.12	group
60.00	52.30	77.00	39.55	1.12	
65.00	36.78	82.81	29.25	1.11	
70.00	25.09	88.48	21.05	1.00	
75.00	16.40	94.01	14.55	1.13	
80.00	10.82	99.39	10.18	1.14	
90.00	4.903	109.69	5.213	2.2	
100.00	3.673	119.37	4.429	1.16	
110.00	5.888	128.44	8.047	0.90	
120.00	9.374	136.94	14.44	0.80	
130.00	14.64	144.93	25.17	0.65	
140.00	18.31	152.48	34.61	0.52	
150.00	22.01	159.68	44.98	0.60	
160.00	24.98	166.60	54.07	0.43	
165.00	25.85	169.99	57.12	0.49	
168.00	26.41	172.01	58.92	1.00	

detected particle at these angles it was necessary to operate without the normal coincidence and mass identification system. Detecting the recoiling helium-3 particle at larger angles was not feasible.

$T(p, {}^3He)n$ center-of-mass differential cross sections are depicted graphically in Fig. 6. The solid line represents cross sections generated by extrapolating the Legendre coefficients of Wilson, Walter, and Fossan[17] to 13.600 MeV. The errors in this process are uncertain. The cross sections of Wilson, Walter, and Fossan were given for the reaction $T(p, n)^3He$ and have been corrected in angle to correspond to the reaction $T(p, {}^3He)n$. [Angles for $T(p, {}^3He)n$ are the 180° compliments of angles for $T(p, n)^3He$.] Error bars are deleted where they are smaller than the plotting dots used.

V. COMPARISON WITH RELATED DATA

A. T(p, p)T Differential Cross Sections at 13.600, 16.230, and 19.480 MeV

As shown in Figs. 1–3 the elastic differential center-of-mass cross sections of $T(p, p)T$ at 13.600, 16.230, and 19.480 MeV, respectively, are compared with the $^3He(p, p)^3He$ data of Hutson *et al.*[9, 10] at the same energies. Several similarities in the cross sections are to be noted. For center-of-mass angles greater than 60°, the $T(p, p)T$ and $^3He(p, p)^3He$ cross sections have the same general shape with minima occurring at the same angles. This minimum in the cross section is located at larger angles as the energy is increased. For angles larger than approximately 60° in the center-of-mass system the $^3He(p, p)^3He$ cross sections are greater than the corresponding $T(p, p)T$ cross sections. The difference between $^3He(p, p)^3He$ and $T(p, p)T$ differential cross sections at large angles decreases as the energy is increased.

At angles less than about 60° in the center-of-mass system the $^3He(p, p)^3He$ differential cross sections are notably less than the corresponding $T(p, p)T$ cross sections and are different in shape. In this angular range the differences between the $^3He(p, p)^3He$ and $T(p, p)T$ differential cross sections may be interpreted as due to increased interference effects between the large Coulomb force in ^3He and the nuclear forces.

At angles greater than about 60° (c.m.), where Coulomb scattering interference effects are not

TABLE IV. $T(p, p)T$ differential cross sections at 19.480 MeV.

θ_{lab} (deg)	σ_{lab} (mb/sr)	$\theta_{c.m.}$ (deg)	$\sigma_{c.m.}$ (mb/sr)	Relative error (%)	Scale error (%)
12.00	397.7	16.04	224.5	0.70	0.77
15.00	387.8	20.04	220.5	0.59	for
20.00	348.0	26.66	200.9	0.57	this
25.00	298.3	33.24	175.6	0.54	group
30.00	241.0	39.76	145.3	0.54	
35.00	187.9	46.21	116.4	0.54	
40.00	142.9	52.57	91.45	0.56	
40.00	144.9	52.57	92.70	0.52	0.68
55.00	55.23	71.09	39.83	0.50	for
60.00	38.91	77.03	29.42	0.54	this
65.00	27.01	82.84	21.48	0.56	group
70.00	18.42	88.52	15.45	0.57	
75.00	12.42	94.05	11.02	0.65	
80.00	8.419	99.42	7.923	0.80	
90.00	4.034	109.72	4.291	1.08	
45.00	107.4	58.85	71.26	0.52	0.68
50.00	77.85	65.03	53.74	0.55	for
60.00	38.63	77.03	29.20	0.57	this
100.00	3.046	119.40	3.675	1.40	group
110.00	4.443	128.47	6.076	1.06	
120.00	7.308	136.97	11.27	0.80	
130.00	10.85	144.95	18.66	0.77	
140.00	14.41	152.50	27.27	0.69	
150.00	17.43	159.69	35.66	0.68	
160.00	19.95	166.61	43.24	0.53	
165.00	20.48	170.00	45.30	0.52	
168.00	21.05	172.01	47.03	1.00	

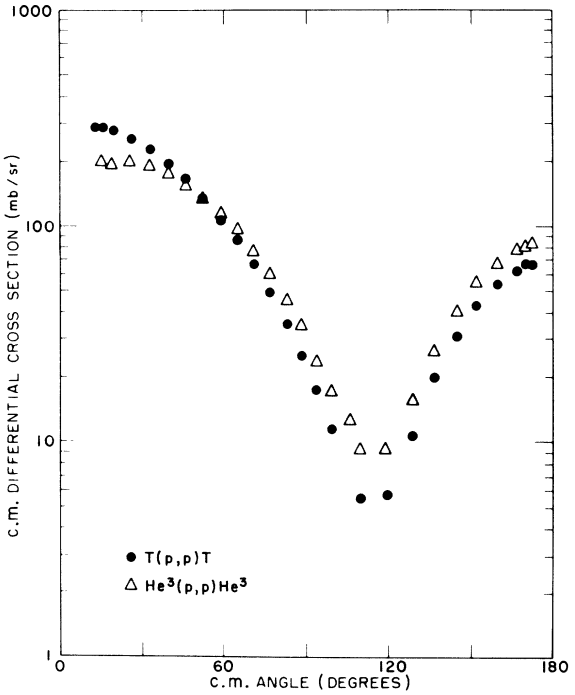

FIG. 1. $T(p, p)T$ and $^3He(p, p)^3He$ data at 13.600 MeV. Our $T(p, p)T$ data (solid circles) are compared with the $^3He(p, p)^3He$ data of Jett *et al.* (see Ref. 10) at 13.600 MeV. Errors are generally less than 1% and are approximately $\frac{1}{4}$ the size of the plotting dots.

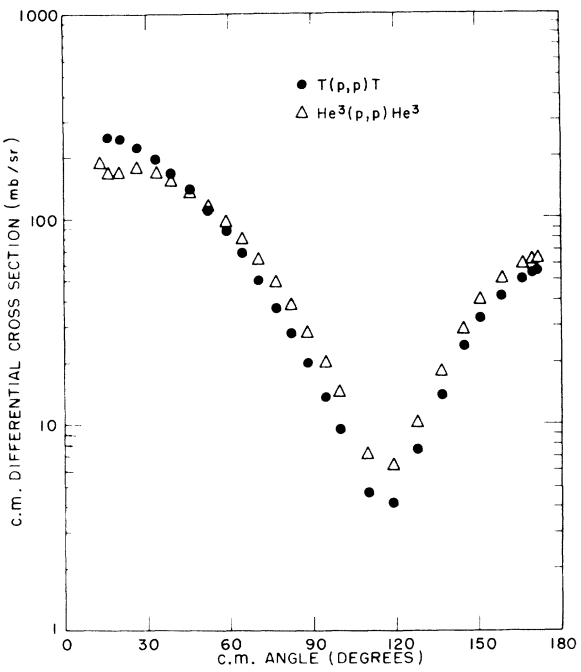

FIG. 2. T(p,p)T and ^{3}He(p,p)^{3}He data at 16.230 MeV. Our T(p,p)T data (solid circles) are compared with the ^{3}He(p,p)^{3}He data of Jett *et al.* (see Ref. 10) at 16.230 MeV. Errors are generally less than 1% and are roughly $\frac{1}{4}$ the size of the plotting dots.

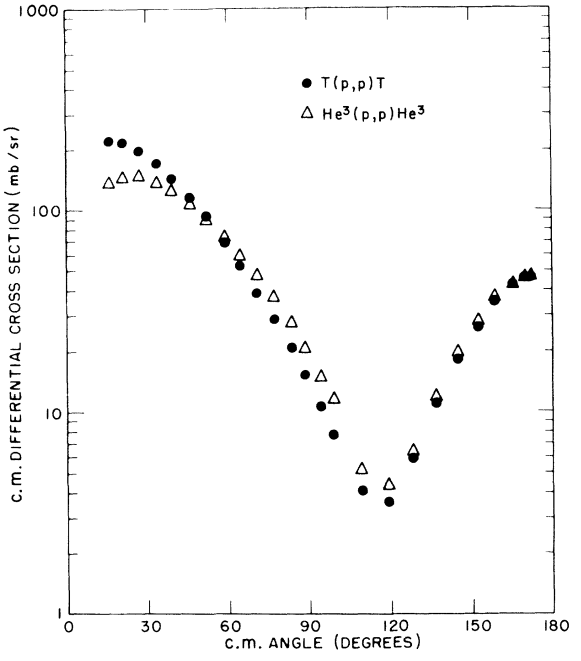

FIG. 3. T(p,p)T and ^{3}He(p,p)^{3}He data at 19.480 MeV. Our data (solid circles) are compared with the data (open triangles) of Jett *et al.* (see Ref. 10). Errors are typically less than 1% and are roughly $\frac{1}{4}$ the size of the plotting dots.

as important, the ^{3}He(p, p)^{3}He differential cross sections are generally larger than the corresponding T(p, p)T differential cross sections. The exceptions are the extreme backward scattering angle data at 19.480 MeV where the T(p, p)T cross sections have become greater than the corresponding ^{3}He(p, p)^{3}He cross sections. Lutz and Anderson[33] have interpreted the cross-section differences of T(p, p)T and ^{3}He(p, p)^{3}He at lower energies as being due to destructive interference between isospin singlet and triplet states in helium 4.

^{3}He(p, p)^{3}He scattering occurs in isospin triplet states having $T_3 = 1$ and $T = 1$ (lithium-4 system). These states have analog states ($T_3 = 0$ and $T = 1$) in the helium-4 system [corresponding to T(p, p)T scattering]. The helium-4 system may also have isospin singlet states ($T_3 = T = 0$) which have no analog states in the lithium-4 system. In other words, ^{3}He(p, p)^{3}He scattering is determined by isospin triplet states, whereas T(p, p)T scattering may be determined by both isospin singlet and triplet states, which might account for differences in the differential cross sections.

However, at 13.600 MeV the apparent differences between ^{3}He(p, p)^{3}He and T(p, p)T differential cross sections can possibly be explained in terms of the different Coulomb energies of the compound nuclei. The assumption is made that the wave number relevant to the nuclear scattering may be

TABLE V. T($\vec{p}$, $\hat{p}$)T proton analyzing power at 13.600 MeV.

θ_{lab}	$\theta_{c.m.}$	A	δA	θ_{lab}	$\theta_{c.m.}$	A	δA
15.00	20.01	−0.012	0.003	90.00	109.66	0.123	0.025
20.00	26.63	−0.032	0.004	97.50	116.98	0.620	0.017
30.00	39.71	−0.052	0.006	105.00	123.97	0.697	0.030
40.00	52.52	−0.098	0.008	105.00	123.97	0.705	0.021
50.00	64.97	−0.158	0.012	120.00	136.92	0.401	0.012
60.00	76.97	−0.226	0.012	140.00	152.47	0.181	0.020
70.00	88.45	−0.299	0.014	150.00	159.67	0.112	0.013
80.00	99.36	−0.265	0.021	160.00	166.60	0.076	0.011

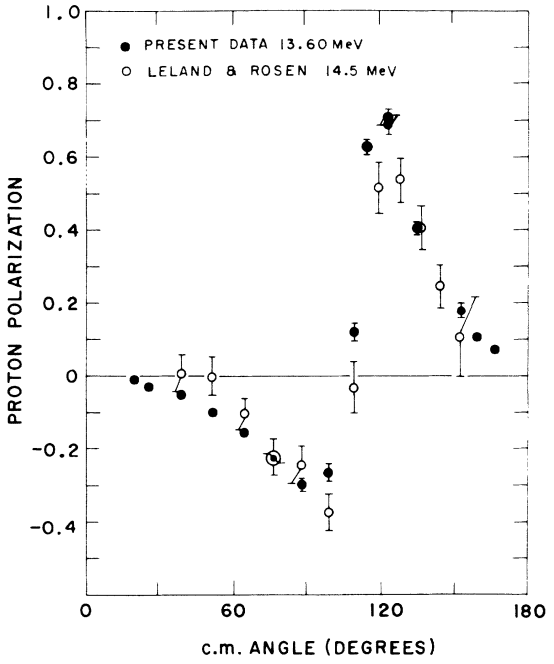

FIG. 4. Proton analyyzing power of $T(\vec{p},\hat{p})T$ at 13.600 MeV. Our data (solid circles) at 13.600 MeV are compared with the corresponding data of Rosen and Leland (see Ref. 6) at 14.5 MeV (open circles). Absolute errors are plotted. Error bars are deleted when exceeded by the size of the plotting dots. The scale error of our data is 1.0%.

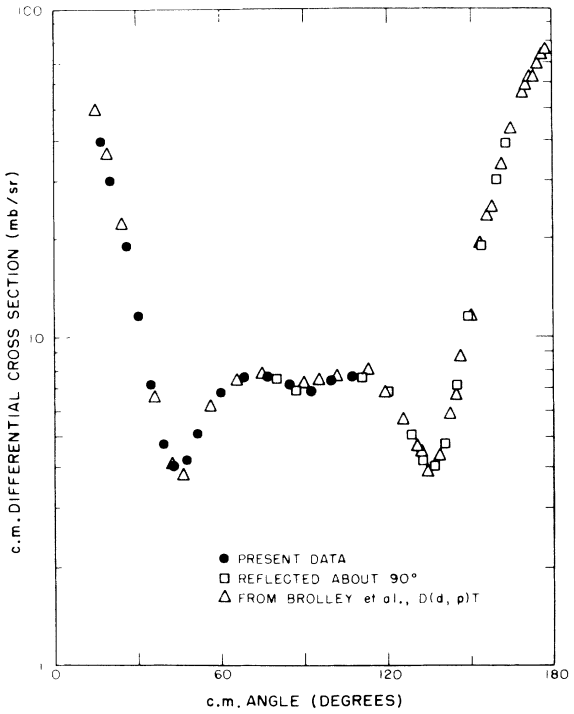

FIG. 5. $T(p,d)D$ and $D(d,p)T$ data at 13.6 MeV. Our $T(p,d)D$ data at 13.600 MeV are plotted with solid circles. Open squares represent our data reflected about 90°. Our relative errors are typically 1.1% and are exceeded by the size of the plotting dots. The $D(d,p)T$ data of Brolley, Putnam, and Rosen (see Ref. 11) at 12.15 MeV have been decreased by a factor of 12.15/12.324 to adjust the cross sections to the corresponding center-of-mass energy. Detailed-balance calculations yield the $T(p,d)D$ data plotted in open triangles. Errors for these data are typically 3 to 4%. Error bars are not shown for these data, but are approximately the size of the triangles.

TABLE VI. $T(p, d)D$ differential cross sections at 13.600 MeV.

θ_{lab} (deg)	σ_{lab} (mb/sr)	$\theta_{c.m.}$ (deg)	$\sigma_{c.m.}$ (mb/sr)	Relative error (%)	Scale error (%)
10.00	126.1	17.45	41.91	1.00	1.24
12.00	95.73	20.94	32.02	1.24	for
15.00	58.96	26.15	19.96	1.42	this
17.50	36.34	30.48	12.45	1.00	group
20.00	21.91	34.80	7.608	1.08	
25.00	11.97	43.40	4.297	1.21	
35.00	19.19	60.36	7.558	0.73	
40.00	19.32	68.68	8.074	0.77	
50.00	15.77	84.87	7.660	0.84	
60.00	13.55	100.25	8.016	0.89	
65.00	12.48	107.54	8.318	1.20	
22.50	15.14	39.11	5.340	0.93	2.0
27.50	12.81	47.67	4.693	1.11	for
30.00	14.94	51.93	5.592	1.05	this
45.00	18.35	76.86	8.225	1.04	group
55.00	14.52	92.68	7.733	1.9	

TABLE VII. $T(p, {}^3He)n$ differential cross sections at 13.600 MeV.

θ_{lab} (deg)	σ_{lab} (mb/sr)	$\theta_{c.m.}$ (deg)	$\sigma_{c.m.}$ (mb/sr)	Relative error (%)	Scale error (%)
12.00	106.0	24.50	26.01	0.89	2.0
15.00	80.56	30.63	20.03	0.89	for
20.00	46.16	40.85	11.80	0.87	entire
25.00	27.72	51.09	7.345	2.2	group
30.00	26.61	61.35	7.379	1.5	
35.00	30.60	71.64	8.974	0.97	
40.00	35.24	81.96	11.05	1.1	
45.00	36.69	92.34	12.46	1.4	
50.00	31.04	102.80	11.6	8.0	

written as

$$k=[2\mu(E_{\text{c.m.}}-E_{\text{Coul}})]^{1/2}/\hbar\,, \tag{1}$$

where μ is the reduced mass, $E_{\text{c.m.}}$ is the center-of-mass energy, E_{Coul} is the Coulomb energy associated with the given compound nucleus.

If one assumes that the Coulomb energy can be calculated using the model of a uniformly charged sphere and noting that differential cross sections are inversely proportional to the square of the wave number, the use of Eq. (1) predicts[27] that the ratio of ^{3}He$(p,p)^3$He to T(p,p)T cross sections should be 1.32 (at 13.6 MeV).

The average ratio of the nine largest-angle cross sections for ^{3}He$(p,p)^3$He and T(p,p)T at 13.600 MeV (where the shapes are approximately the same) is found experimentally to be 1.31. The assumptions in this calculation are crude (especially for the Coulomb energy), but the result is suggestive that the nuclear scattering amplitudes are similar for the two processes at this energy.

Additional information on this idea comes from a comparison of the analyzing powers. Tombrello[3] indicates that the ^{3}He$(\vec{p},\hat{p})^3$He and T$(\vec{p},\hat{p})$T proton analyzing powers are nearly independent of the wave number k, and depend almost entirely upon the scattering matrix elements. In Fig. 7, T$(\vec{p},\hat{p})$T and Tivol's ^{3}He$(\vec{p},\hat{p})^3$He analyzing-power data[8] are compared and are seen to be similar.

The near identity of the ^{3}He$(\vec{p},\hat{p})^3$He and T$(\vec{p},\hat{p})$T proton analyzing powers and the similarity in the ^{3}He$(p,p)^3$He and T(p,p)T differential cross sections after accounting for the dissimilar Coulomb energies of the compound nuclei suggests that near 30 MeV in the helium-4 system the scattering is dominated by $T=1$ (isospin triplet) states. (30 MeV in the helium-4 system corresponds to a proton laboratory energy of 13.6 MeV.)

In Fig. 8 our data are compared with the disputed T(p,p)T elastic scattering data of Vanetsian and Fedchenko[5] at 19.48 MeV. It may be seen that significant differences in shape exist between their data and ours, with numerical differences being as much as 50 or 60% in some cases (see Introduction).

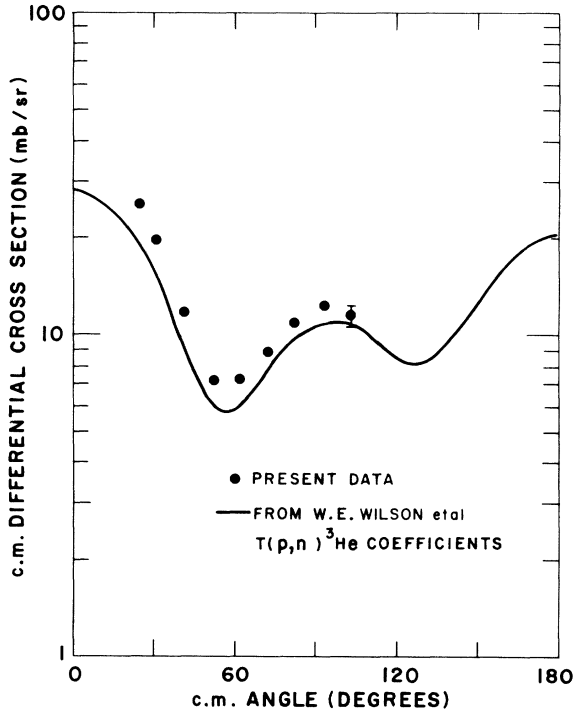

FIG. 6. T$(p,{}^3\text{He})n$ center-of-mass differential cross sections at 13.600 MeV. Solid circles represent our data. Errors are typically 1.1% and are exceeded by the size of the plotting dots used. The solid line was generated by extrapolating the T$(p,n)^3$He Legendre coefficients of Wilson, Walter, and Fossan (see Ref. 17) to 13.6 MeV, and converting the center-of-mass angle to correspond to T$(p,{}^3\text{He})n$.

B. T$(\vec{p},\hat{p})$T Proton Analyzing Power at 13.600 MeV

In Fig. 4 our T$(\vec{p},\hat{p})$T proton analyzing power data at 13.600 MeV is graphically compared with

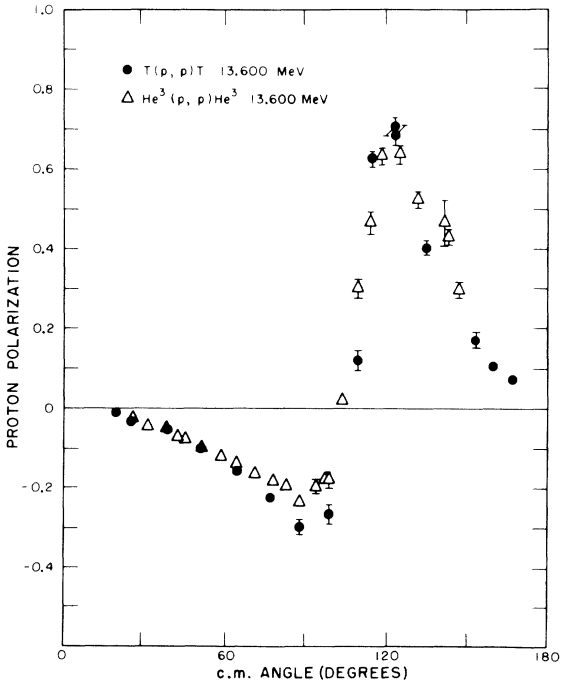

FIG. 7. Comparison of T$(\vec{p},\hat{p})$T and ^{3}He$(\vec{p},\hat{p})^3$He proton analyzing power at 13.600 MeV. Our T$(\vec{p},\hat{p})$T data (solid circles) are compared with the ^{3}He$(\vec{p},\hat{p})^3$He data (open triangles) of Tivoli (see Ref. 8) at 13.6 MeV.

the $T(\vec{p},\hat{p})T$ analyzing power data of Rosen and Leland[7] at 14.5 MeV. These two sets of data are in general agreement, though the data of Rosen and Leland was obtained by a double-scattering experiment without the benefit of a high-intensity polarized ion source and displays greater statistical errors. Rosen and Leland's data imply that the proton analyzing power is perhaps greater than zero in the angular region less than 50° in the center-of-mass system. By comparison with our data it is believed that the proton analyzing power remains negative for angles less than 90° c.m.

In Fig. 7 our $T(\vec{p},\hat{p})T$ proton analyzing power data at 13.600 MeV is compared with the $^3He(\vec{p},\hat{p})^3He$ analyzing power data of Tivol[8] at 13.600 MeV. Except for a difference in absolute normalization, $^3He(\vec{p},\hat{p})^3He$ and $T(\vec{p},\hat{p})T$ proton analyzing powers appear to have the same angular dependence. This implies that polarization effects of this order of magnitude are charged independent. Jarmie and Jett[31] had experienced difficulty in fitting Tivol's data at angles greater than 150° in their phase-shift analysis, and they believed that Tivol's data for angles greater than 150° c.m. were in error. Walter[22] measured the neutron analyzing power for $T(\vec{n},\hat{n})T$ at 22.1 MeV and compared his data with Tivol's $^3He(\vec{p},\hat{p})^3He$ analyzing-power measurements in the mirror nuclear system at 21.3 MeV. Comparison of Walter's $T(\vec{n},\hat{n})T$ data and Tivol's $^3He(\vec{p},\hat{p})^3He$ data indicates that Tivol's data differs with Walter's and our data by a similar normalization discrepancy of about 9%. However, recent data of Jarmie and Jett[31] do not show Tivol's $p+^3He$ data at 13.6 MeV to be incorrect, and the situation remains unresolved.

C. $T(p,d)D$ Reaction Differential Cross Sections at 13.600 MeV

$T(p,d)D$ reaction differential cross sections at 13.600 MeV are presented in Fig. 5. For comparison of the 90° symmetry due to identical particles in the outgoing channel, the reflected data is also presented. A proton laboratory energy of 13.600 MeV is equivalent to a proton-triton center-of-mass energy of 10.195 MeV. The mass difference between the incoming and outgoing channels in the $T(p,d)D$ reaction provides a Q value of $Q=-4.033$ MeV. Following the reaction $T(p,d)D$ the deuteron-deuteron center-of-mass energy is 6.162 MeV, which is equivalent to a deuteron laboratory energy of 12.324 MeV for the reaction $D(d,p)T$. Brolley, Putnam, and Rosen[11] measured the reaction $D(d,p)T$ at 12.15 ± 0.15 MeV with errors of 3 to 4%. Their data has been reduced by the ratio of 12.15 : 12.324 to correct to first order for the energy difference, and used to generate $T(p,d)D$ reaction cross sections at a proton laboratory energy of 13.600 MeV by the principle of detailed balance.[12] The $T(p,d)D$ data thus generated from the data of Brolley, Putnam, and Rosen are compared graphically with our $T(p,d)D$ data at 13.600 MeV in Fig. 5, and is in good agreement. The good agreement of the $D(d,p)T$ data of Brolley, Putnam, and Rosen and our $T(p,d)D$ data verifies the invariance of nuclear forces under time reversal. This is quantitatively stated from a statistical comparison of the two sets of data. If $1+\Delta$ is equal to the ratio (theirs to ours) of cross sections (detail-balance factors taken into account; see Ref. 34), then preliminary calculations give Δ to be on the order of 0.03 compatible with the 3–4% errors on the $D(d,p)T$ data. Detailed calculations are in progress.

As expected, $T(p,d)D$ reaction cross sections are approximately an order of magnitude less than the elastic $T(p,p)T$ differential cross sections.

D. $T(p,{}^3He)n$ Reaction Differential Cross Sections at 13.600 MeV

Our $T(p,{}^3He)n$ reaction differential cross sections at 13.600 MeV are presented in Fig. 6 along

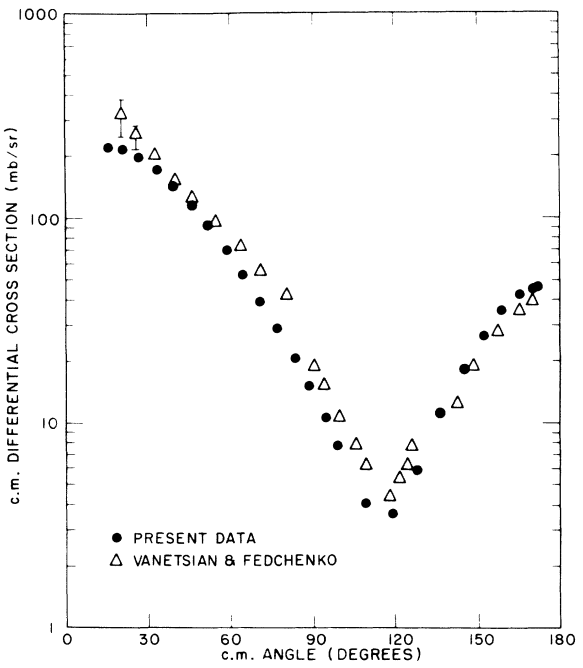

FIG. 8. Comparison of $T(p,p)T$ data at 19.480 MeV. Our data (solid circles) are compared with the $T(p,p)T$ data (open triangles) of Vanetsian and Fedchenko (see Ref. 5) at 19.48 MeV. Errors for our data are typically less than 1%. Numerical values for the data and errors of Vanetsian and Fedchenko are not available. Their data points were transcribed from a graph, and numerically differ by as much as 50% from our values.

with data obtained from Wilson, Walter, and Fossan's[17] measurements of $T(p,n)^3He$. Wilson, Walter, and Fossan measured the relative neutron cross sections with a stilbene detector with pulse-shape discrimination, and then normalized these data to the 0° cross section obtained by a proton-recoil detector. Their estimation of the normalization accuracy is ±15%. The line shown in Fig. 6 was obtained by extrapolating Wilson, Walter, and Fossan's Legendre coefficients to an energy of 13.6 MeV and generating an angular distribution from the summation of Legendre polynomials. The neutron center-of-mass angle θ was replaced by $180-\theta$ to correspond to the center-of-mass angle of the recoiling helium-3 particle. The errors involved in extrapolating the Legendre coefficients to higher energy are uncertain. However, comparison of their cross-section measurements with our equivalent absolute cross-section measurements indicates that their cross sections should be multiplied by a factor of 1.19 ± 0.05.

The $T(p,{}^3He)n$ differential cross sections are also approximately an order of magnitude less than the elastic $T(p,p)T$ differential cross sections.

VI. PHASE-SHIFT RESULTS AND INTERPRETATION

A. T(p, p)T Elastic Scattering and Analyzing Power

Our $T(p,p)T$ elastic scattering and $T(\vec{p},\hat{p})T$ proton analyzing-power data at 13.600 MeV were analyzed by Dodder's[4] energy-independent reaction-matrix phase-shift analysis program. The program was capable of arriving at solutions in a reasonable amount of machine time for a maximum angular momentum L value of 3. Initial phase-shift guesses were obtained in two ways. Corresponding phase-shift solutions[3,10] for $^3He(p,p)^3He$ data were put in as starting guesses because of the similarity of $T(p,p)T$ and $^3He(p,p)^3He$ data, and alternately a deck of random numbers between −180 and +180° was used for input phases.

The solutions which started from a known set of $^3He(p,p)^3He$ phase shifts usually converged fairly quickly (~25 iteractions) to values of χ^2 per point of about 1.0, with corresponding values of χ^2 per degree of freedom (weighted variance) of about 2. These were distinct solutions which graphically appeared to fit the elastic scattering and polarization data equally well, but offered large discrepancies in their predictions of the observables A_{xx}, A_{yy}, A_{xz}, D_1, D_2, and R_1, for which no data exist. These solutions predicted the polarization of the recoiling particle P_2 to be similar in shape to the measurements of P_1, the polarization of the detected particle. The solutions arrived at from Tombrello's $^3He(p,p)^3He$ phase shifts[3] and from Jarmie and Jett's[31] α and β $^3He(p,p)^3He$ phase-shift solutions are presented in Table VIII. The phase-shift notation used is Blatt-Biedenharn nuclear notation.[35] The ease with which different solutions are obtained and the frequently unphysical values obtained for the phases indicate that more data are needed before significant solutions can be found.

The solutions which originated from random starts encountered three types of difficulty: (1) One or more phase shifts would asymptotically approach ±90°, causing unreasonably large values of the corresponding elements of the Q matrix ($Q=\tan\delta$). Artificial displacement of this phase shift to the other side of 90°, or otherwise changing its value usually did not circumvent the problem for more than a few iterations. (2) In the diagonalization of the matrix which is used to determine the size of the step to be taken in a given iteration, the eigenvalues frequently became large (greater than 10^{13}), causing the iteration step direction to become disoriented. (3) Numerous spurious solutions were generated having χ^2 per point values between 2 and 100 which did not fit the data well, but which were local minima in the χ^2 surface of parameter space. Artificial displacement of an unreasonable parameter (such as an unreasonably large F-wave phase shift) usually produced a different variation of one or more of the above three types of problems.

B. Related Mass-4 Single-Channel Data

It was originally anticipated that single-channel phase-shift solutions would be useful initial values for the analysis of the two-channel reactions. For example, separate phase-shift solutions for $T(p,p)T$ and $D(d,d)D$ single-channel data would be used as initial parameter guesses for the two-channel analysis of $T(p,p)T$, $T(p,d)D$, and $D(d,d)D$. Available single-channel $D(d,d)D$ data,[36] and $^3He(n,n)^3He$[37,38] at nearby energies were analyzed and several marginally satisfactory solutions obtained.

Using a maximum L value of 2, the $D(d,d)D$ data[36] yielded a variety of solutions having values of χ^2 per point of 0.95 and χ^2 per degree of freedom of 3.15. The scatter of the available data points and the associated errors were such that χ^2 was fairly insensitive to changes in the phase shifts. In other words, local minima in the χ^2 surface were not located. Many interactions and large excursions across parameter space did not locate significant solutions, and the solutions thus

obtained contained large errors in the phase shifts indicating that like solutions could be obtained with large differences in the phase shifts. Analysis of the same data using L values of 3 produced slight improvement of χ^2 per point to values of 0.89, though χ^2 per degree of freedom was increased to 8.9 by the increased number of available parameters. Visual comparison of the obtained solutions and the available data indicates a good fit, though the available data is inadequate to distinguish spurious solutions.

Existing ^{3}He$(n,n)^3$He elastic scattering data by Antolkovic *et al.*[37] and neutron polarization data by Büsser *et al.*[38] were similarly analyzed yielding a variety of solutions having values of χ^2 per point of about 0.5, and χ^2 per degree of freedom of between 2.0 and 3.0. Visual comparison of the existing data appears good, but the data is over restricted angular ranges, making it easier to fit.

C. Two-Channel Phase-Shift Analysis

Simultaneous two-channel phase-shift analysis was attempted of data for the reaction combinations [T(p,p)T, T(p,d)D, D(d,d)D], [T(p,p)T, T$(p,n)^3$He, ^{3}He$(n,n)^3$He], and [^{3}He$(n,n)^3$He, ^{3}He(n,d)D, and D(d,d)D]. The previous single-channel phase-shift solutions as well as random guesses were used as starting values for the appropriate parameters. For starting the two-channel problems the single-channel solutions offered little improvement over random initial parameter guesses. The two-channel analysis used L values of 2 in all channels, which provided 42 parameters for the analysis of the T-p ^{3}He-n data, and 43 parameters for the T-p n-d, and the ^{3}He-n D-d analysis. The CDC 6600 computer used typically required approximately 25 min to reduce the value of χ^2 per degree of freedom from about 2000 to about 400. The analysis was quite susceptible to the 90° phase-shift problems associated with the single-channel analyses, and computing was done in time steps of 2 min to allow manual displacement of the offending phase shifts from 90°.

The simultaneous two-channel analyses were also susceptible to the following problem: When local minima in χ^2 were obtained in either of the elastic-channel predictions, the program was unable to improve agreement between calculated and measured data in the other reaction channels. Using starting values obtained from the single-channel analysis, the typical end product of the two-channel analysis was a mediocre agreement with the elastic-channel data, and a poor agreement with the reaction-channel data. Further iterations produced either a negligible reduction in χ^2, or resulted in the 90° confusion common to the single-channel analyses. In summary, attempts to find a meaningful two-channel solution failed.

TABLE VIII. T(p,p)T phase shifts at 13.600 MeV.

Starting set $^{2S+1}L_J$	α		β		Tombrello	
	δ (deg)	Error (deg)	δ (deg)	Error (deg)	δ (deg)	Error (deg)
$^3S_1$	−89.5	0.8	−119.6	3.8	52.8	6.5
$^3S_1 - {}^3D_1$	85.6	6.0	−23.6	4.1	19.4	12.8
$^3D_1$	−53.0	3.9	3.2	3.7	−1.8	12.4
$^3P_2$	81.5	18.8	69.7	3.0	42.1	5.9
$^3P_2 - {}^3F_2$	−48.0	95.4	−43.6	5.2	15.3	5.7
$^3F_2$	10.6	29.3	12.8	3.1	−2.0	7.5
$^3P_1$	51.3	22.5	21.4	4.3	55.0	12.3
$^3P_1 - {}^1P_1$	3.9	14.6	8.1	5.7	40.5	17.2
$^1P_1$	−14.7	24.8	57.3	7.0	61.2	12.1
$^3P_0$	69.9	58.5	73.0	5.8	−18.7	19.9
$^3D_3$	5.1	11.4	−1.7	1.9	14.7	4.1
$^3D_2$	6.0	25.7	−0.2	3.5	6.0	7.8
$^3D_2 - {}^1D_2$	6.2	11.4	3.3	1.9	−3.3	4.0
$^1D_2$	4.3	5.4	9.6	2.4	−34.5	2.6
$^3F_4$	3.7	5.3	−9.7	2.0	−2.2	1.7
$^3F_3$	1.0	15.9	−1.5	2.0	−5.1	3.6
$^3F_3 - {}^1F_3$	−0.2	9.0	4.4	1.9	−2.5	2.3
$^1F_3$	−5.3	7.3	6.9	1.6	−4.5	2.3
$^1S_0$	−6.2	49.4	−112.8	9.6	−100.7	11.7
Weighted variance	1.93		4.1		3.0	

D. Simultaneous Three-Channel Phase-Shift Analyses

Simultaneous phase-shift analysis using data for the reactions $T(p,p)T$, $T(p,d)D$, $T(p,n)^3He$, $^3He(n,n)^3He$, $^3He(n,d)D$, and $D(d,d)D$ was attempted with the hopes that the additional data would decrease the ambiguity of possible phase-shift solutions. For a maximum L value of 2, this program contained 87 parameters, and encountered an order of magnitude more difficulty of calculation than the two-channel analyses. The three-channel analysis did not succeed in locating even local minima in the χ^2 surface, and hence was wholly inconclusive. A simultaneous three-channel phase-shift solution for the mass-4 system would be valuable for the understanding of the nuclear forces. Success in a phase-shift analysis of this problem awaits more data, improved in accuracy and varied in observable types (such as spin correlations). Improvements in the computer program would be also very desirable.

ACKNOWLEDGMENTS

We are indebted to the P-9 (Los Alamos Scientific Laboratory) staff for the operation of the accelerators, to the accelerator operators for their patience and perserverance, to L. L. Catlin and J. C. Martin for their technical assistance. Thanks and appreciation are due Joseph L. McKibben, Gerald G. Ohlsen, and George P. Lawrence for the assistance and labor expended in the operation of the polarized ion source.

We would like to thank Jules Levin and Martin Kellogg for assistance in communicating with the on-line computer. Special appreciation is due D. C. Dodder for generously providing the use of his phase-shift-analysis computer program, and especially due Mrs. Kathleen Witte for assistance in its operation. F. S. Dietrich and W. E. Meyerhof kindly sent us their $D(d,n)$ Legendre coefficients.

---

*Work performed under the auspices of the U. S. Atomic Energy Commission.

†Now at EG&G, Los Alamos, New Mexico 87544.

[1]W. E. Meyerhof and J. N. McElearney, Nucl. Phys. 74, 533 (1965).

[2]C. Werntz, Phys. Rev. 133, B19 (1964).

[3]T. A. Tombrello, Phys. Rev. 138, B40 (1965).

[4]D. C. Dodder, private communication.

[5]R. A. Vanetsian and E. D. Fedchenko, At. Energ. (USSR) 2, 123 (1957) [transl.: Soviet J. At. Energy 2, 141 (1957).

[6]L. Rosen and W. T. Leland, unpublished; and private communication.

[7]L. Rosen and W. T. Leland, Phys. Rev. Letters 8, 379 (1962).

[8]W. F. Tivol, University of California Radiation Laboratory Report No. UCRL-18137, 1968 (unpublished).

[9]R. L. Hutson and N. Jarmie, Bull. Am. Phys. Soc. 14, 21 (1969).

[10]J. H. Jett, R. L. Hutson, J. L. Detch, Jr., and N. Jarmie, Bull. Am. Phys. Soc. 15, 1661 (1970); R. L. Hutson, N. Jarmie, J. L. Detch, and J. H. Jett, to be published.

[11]J. E. Brolley, Jr., T. M. Putman, and L. Rosen, Phys. Rev. 107, 820 (1957).

[12]W. S. C. Williams, *Introduction to Elementary Particles* (Academic Press Inc., New York, 1961), p. 89 ff.

[13]G. F. Bogdanov, N. A. Vlasov, C. P. Kalinin, B. V. Rybakov, L. N. Samoilov, and V. A. Sidorov, *Nuclear Reactions at Low and Intermediate Energy* (in Russian) (Akad. Nauk SSSR, Moscow, 1958), p. 7.

[14]G. F. Bogdanov, N. A. Vlasov, C. P. Kalinin, B. V. Rybakov, L. N. Samoilov, and V. A. Sidorov, Zh. Eksperim. i Teor. Fiz. 36, 633 (1959) [transl.: Soviet Phys.–JETP 9, 440 (1959)].

[15]M. D. Goldberg, J. D. Anderson, J. P. Stoering, and C. Wong, Phys. Rev. 122, 1510 (1961).

[16]M. D. Goldberg, Brookhaven National Laboratory Report No. BNL-6765, 1963 (unpublished).

[17]W. E. Wilson, R. L. Walter, and B. D. Fossan, Nucl. Phys. 27, 421 (1961).

[18]F. S. Dietrich and W. E. Meyerhof, private communication.

[19]J. D. Seagrave, in *Proceedings of the Symposium on Few Body Problems, Light Nuclei, and Nuclear Interactions, Brela, Yugoslavia, 26 June–5 July 1967* (Gordon and Breach, Science Publishers, Inc., New York, 1969).

[20]H. H. Barschall, in *Proceedings of the Second International Symposium on Polarization Phenomena of Nucleons, Karlsruhe, Germany, 1965* (Birkhauser Verlag, Basel, Germany, 1966), p. 393.

[21]R. L. Walter, W. Benenson, P. S. Dubbeldam, and T. H. May, Nucl. Phys. 30, 292 (1962).

[22]R. K. Walter, Los Alamos Scientific Laboratory Report No. LA-4334 (unpublished); R. K. Walter, J. C. Hopkins, E. Kerr, J. Martin, A. Niiler, J. D. Seagrave, R. Sherman, D. Dixon, Phys. Letters 30B, 626 (1969); see also Ref. 25.

[23]N. V. Alekseev, U. R. Arifhanov, N. A. Vlasov, V. V. Davydov, and L. N. Samoilov, Zh. Eksperim. i Teor. Fiz. 45, 1416 (1963) [transl.: Soviet Phys.–JETP 18, 979 (1964).

[24]W. E. Meyerhof and T. A. Tombrello, Nucl. Phys. A109, 1 (1968).

[25]J. L. Detch, Jr., J. H. Jett, and N. Jarmie, in Proceedings of the Third International Symposium on Polarization Phenomena, Madison, Wisconsin, 1970 (to be published); Los Alamos Scientific Laboratory Report No. LA-4465-MS (unpublished).

[26]J. L. Detch, Jr., R. L. Hutson, and N. Jarmie, Bull. Am. Phys. Soc. 15, 22 (1970).

[27]J. L. Detch, Jr., Ph.D. thesis, University of Wyoming, 1970 (unpublished); Los Alamos Scientific Laboratory Report No. LA-4576 (unpublished).

[28]N. Jarmie, J. H. Jett, J. L. Detch, Jr., and R. L. Hutson, Phys. Rev. C 3, 10 (1971).
[29]G. P. Lawrence, G. G. Ohlsen, J. L. McKibben, Phys. Letters 28B, 594 (1969).
[30]G. R. Satchler, L. W. Owen, A. J. Elwyn, G. L. Morgan, and R. L. Walter, Nucl. Phys. A112, 1 (1968), and references therein.
[31]N. Jarmie and J. H. Jett, private communication.
[32]R. A. Arndt, L. D. Roper, and R. L. Shotwell, to be published.
[33]H. J. Lutz and J. D. Anderson, University of California Radiation Laboratory Report No. UCRL-14568 (unpublished), p. 3.
[34]E. M. Henley, Ann. Rev. Nucl. Sci. 19, 367 (1969).
[35]J. M. Blatt and L. L. Biedenharn, Rev. Mod. Phys. 24, 258 (1952).
[36]J. E. Brolley, T. M. Putman, L. Rosen, and L. Stewart, Phys. Rev. 117, 1307 (1960).
[37]B. Antolković, M. Cerineo, G. Paić, P. Tomas, V. Ajdacić, B. Lalović, W. T. H. van Oers, and I. Slaus, Phys. Letters 23, 477 (1966).
[38]F. W. Büsser, H. Dubenkropp, F. Niehergall, and K. Sinram, Nucl. Phys. A129, 666 (1969).

PHYSICAL REVIEW C VOLUME 4, NUMBER 1 JULY 1971

Λ Binding Energy for the $2s$-$1d$-Shell Hypernuclei. I. $18 \leqslant A \leqslant 21$*

T. Y. Lee, S. T. Hsieh, W. W. Yeh, and C. T. Chen-Tsai
Institute of Physics, Tsing Hua University, Hsinchu, Taiwan, China
(Received 6 January 1971)

The Λ binding energies of the $2s$-$1d$-shell hypernuclei with mass number between 18 and 21 are calculated, using the results of a shell-model calculation for the $1p$-shell hypernuclei previously carried out by the authors.

1. INTRODUCTION

Recently, a great deal of effort has been made in the theoretical calculation of the potential-well depth parameter for a Λ particle in nuclear matter.[1] The "experimental value" for this parameter of approximately[2] 30 MeV has been estimated from the selective binding-energy data of the heavy spallation hypernuclei with mass number ranging from 35 to 100, based on the extrapolation of the binding-energy formula from a uniform model[3] to the heaviest experimentally identified $1p$-shell hypernucleus, i.e., $^{13}_{\Lambda}$C. However, it is well known that the surface effects for the ^{12}C nucleus is quite large and one may not be justified in applying this formula. Therefore, a more accurate determination of this parameter should be made via the binding energies of the hypernuclei of intermediate mass.

Unfortunately, the experimental information about the $2s$-$1d$-shell hypernuclei ($18 \leqslant A \leqslant 41$) is nonexistent. Nevertheless, using the results of our previous shell-model calculation for the $1p$-shell hypernuclei,[4] we are able to calculate the binding energies of the $2s$-$1d$-shell hypernuclei. The calculation, therefore, will not only facilitate the future experimental identification of these nuclides, but also provide, one may hope, a better estimate for the "experimental value" of the potential-well depth parameter.

Because of the difference in computational procedure, we will consider in the present paper only those $2s$-$1d$-shell hypernuclei with mass number between 18 and 21, leaving the calculation for those with mass number larger than 21 to be presented in subsequent papers. In Sec. 2, the strengths of the phenomenological potentials described in Ref. 4 are computed and used in the calculation of the two-body Λ-N potential integrals in the $2s$-$1d$ shell and the binding energies of the $2s$-$1d$-shell hypernuclei. In Sec. 3, the results of the calculation are discussed.

2. COMPUTATIONAL PROCEDURE

Following the method of computation of the binding energy for the $1p$-shell hypernuclei,[4] the binding energy for a given $2s$-$1d$-shell hypernuclei is obtained by the diagonalization of the energy matrices for various isospin T and spin J_Λ. These matrices consist of elements which are the sum of matrix elements of the interaction between nucleons in the $2s$-$1d$ shell, the interaction between the Λ particle and the ^{16}O core, and the interaction between the Λ particle and the nucleons in the $2s$-$1d$ shell.

The core nuclei with $17 < A \leqslant 20$ have been described by Arima *et al.*[5] in a shell model in which the ^{16}O core is assumed to be inert and the nucleons in the unfilled shells occupy only the $2s_{1/2}$ and $1d_{5/2}$ shells (the $2s_{1/2}$ shell is 0.871 MeV above the $1d_{5/2}$ shell). The matrix elements of the interac-